

## Dipole-dipole interaction and its concentration dependence of magnetic fluid evaluated by ac hysteresis measurement

Satoshi Ota<sup>1</sup>, Tsutomu Yamada<sup>1</sup>, and Yasushi Takemura<sup>1, a)</sup>

<sup>1</sup> *Department of Electrical and Computer Engineering, Yokohama National University, Yokohama 240-8501, Japan.*

a) Electronic mail: takemura@ynu.ac.jp

### **Abstract**

Magnetic nanoparticles (MNPs) are used as therapeutic and diagnostic tools, such as for treating hyperthermia and in magnetic particle imaging, respectively. Magnetic relaxation is one of the heating mechanisms of MNPs. Brownian and Néel relaxation times are calculated conventional theories; however, the influence of dipole–dipole interactions has not been considered in conventional models. In this study, water-dispersed MNPs of different concentrations and MNPs fixed with an epoxy bond were prepared. Dc and ac hysteresis loops for each sample were measured. With respect to both dc and ac hysteresis loops, magnetization decreased with increases in MNP concentration because of inhibition of magnetic moment rotation due to dipole–dipole interactions. Moreover, intrinsic loss power (ILP) was estimated from the areas of the ac hysteresis loops. The dependence of ILP on the frequency of the magnetic field was evaluated for each MNP concentration. The peak frequency of ILP increased with decreases in MNP concentration. These peaks were due to Brownian relaxation, as they were not seen with the fixed sample. This indicates that the Brownian relaxation time became shorter with lower MNP concentration, because the weaker dipole–dipole interactions with lower concentrations suggested that the magnetic moments could rotate more freely.

## I. INTRODUCTION

Magnetic hyperthermia and magnetic particle imaging (MPI) using magnetic nanoparticles (MNPs) are effective tools in cancer therapy and diagnostics, respectively [1, 2]. Integrative therapeutic and diagnostics application is called theranostics [3-5], and the evaluation of magnetic relaxation properties is necessary for designing materials that promote both hyperthermia and MPI signal volume. Magnetic relaxation loss is one of the heating mechanisms of MNPs. Magnetic relaxation is characterized by two distinct models: Brownian relaxation occurs through particle rotation, and Néel relaxation occurs through magnetic moment rotation. The Brownian and Néel relaxation times,  $\tau_B$  and  $\tau_N$ , respectively, are given by the following equations [6, 7]:

$$\tau_B = \frac{3\eta V_H}{k_b T} \quad (1)$$

$$\tau_N = \frac{\sqrt{\pi}}{2} \tau_0 \frac{\exp\left(\frac{KV_M}{k_B T}\right)}{\sqrt{\frac{KV_M}{k_B T}}} \quad (2)$$

where  $\eta$ ,  $V_H$ ,  $k_B$ ,  $T$ ,  $\tau_0$ ,  $K$ , and  $V_M$  are the viscosity of the suspended fluid, the hydrodynamic volume of MNPs, the Boltzmann constant  $1.38 \times 10^{-23}$  J/K, the temperature in Kelvin, the attempt time of  $\sim 10^{-9}$  s, the magnetocrystalline anisotropy constant, and the volume of the magnetic core, respectively. Moreover, the effective relaxation time  $\tau$  is described by the following equation, because Brownian and Néel relaxations occur in parallel [6, 7].

$$\frac{1}{\tau} = \frac{1}{\tau_B} + \frac{1}{\tau_N} \quad (3)$$

The effective relaxation time can be evaluated by measuring the frequency dispersion of ac susceptibility in MNPs. In particular, at the peak frequency in the imaginary part of the susceptibility, heat efficiency is the highest [8]. This peak frequency is represented by  $f = (2\pi\tau)^{-1}$ . It is indicated that magnetic relaxation is influenced on the primary and hydrodynamic size and anisotropy of MNPs. The model of MNPs has been evaluated to optimize the heating property [9]. Evaluation of the effective relaxation time by the measurement of the imaginary part of susceptibility has been conducted [8, 10-12]. On the other hand, the effective frequency for heat dissipation can be estimated from the measurement of the dependency of intrinsic loss power (ILP) on frequency. ILP is intrinsic heat dissipation, independent of the applied field, which is calculated from specific loss power (SLP) [13]. SLP was the mass power dissipation, which was derived from a calorimetric measurement [7]. SLP is written in terms of the imaginary part of susceptibility  $\chi''$  as [6, 14]:

$$SLP = \frac{\mu_0 \pi \chi'' f H^2}{\rho} \quad (4)$$

where  $\mu_0$ ,  $f$ ,  $H$ , and  $\rho$  are the permeability of free space, frequency, amplitude of the magnetic field, and the mass density of the MNPs, respectively. Furthermore, ILP is given as follows [13]:

$$ILP = \frac{SLP}{f H^2} \quad (5)$$

For higher concentration of MNPs, magnetization reversal is inhibited because the rotation of magnetic moment is blocked by dipole–dipole interactions. Dipole–dipole interaction dependence on MNP concentration can be assessed by measurement of dc hysteresis loops, imaginary part of susceptibility, and SLP estimated from calorimetric measurements [15–19]. In this study, water-dispersed MNPs in different concentrations and MNPs fixed with an epoxy bond were prepared. The dc and ac hysteresis loops in the frequency range of 1–500 kHz were measured for each sample. Moreover, the dependence of ILP on frequency was estimated from the areas of the ac hysteresis loops.

## II. Materials and methods

### A. Materials

A water-based magnetite nanoparticle, M-300, was purchased from Sigma Hi-Chemical Inc.; The primary and hydrodynamic diameters were  $11 \pm 3$  nm and  $52 \pm 15$  nm, respectively. MNPs were coated with the surfactant of  $\alpha$ -olefin sulphonic acid sodium.

### B. Sample preparation

Both liquid and fixed samples were prepared. MNPs were dispersed in water in varying concentrations to prepare the liquid samples. The concentrations of the MNPs in the liquid samples were 37, 120, 180, 290, and 370 mg-Fe/ml. The concentration of MNPs was estimated using dried sample by calculation using the weight ratio among Fe, Fe<sub>3</sub>O<sub>4</sub>, and surfactant. The concentration of MNPs was high for hyperthermia treatment. However, in this study, evaluation in the higher concentration was conducted for the confirmation of particle–particle interaction to use MNPs as heat source for hyperthermia. Furthermore, MNPs fixed with epoxy bond were used as the fixed sample; the concentration of the MNPs in the fixed sample was 37 mg-Fe/ml. The dispersion state of the fixed sample was not confirmed.

### C. Measurement of ac and dc hysteresis loops

The dc hysteresis loops were measured using a vibrating sample magnetometer in a dc magnetic field of 0–4 kA/m. The ac hysteresis loops were measured at frequencies of 1–500 kHz under an ac magnetic field of amplitude 4 kA/m. The exciting coil was a 70-turn water-cooled solenoid with a diameter of 16.3 mm [20].

## III. Results and Discussion

### A. Dc hysteresis loops

Figure 1 shows the dependence of dc hysteresis loops on MNP concentration in the liquid sample. The hysteresis areas of the dc hysteresis loops in the liquid sample were marginal. In contrast, MNPs in the fixed sample showed anisotropy (Fig. 2), and the measured MNPs showed ferromagnetism. Magnetization of the fixed sample, which has no particle rotation, was lower than that of the liquid samples. This indicates that the reversal of magnetization in the liquid samples was due to rotation of both magnetic moments and particles. Thus, the reversal of magnetization showed little anisotropic behavior in the liquid samples. Magnetization decreased with MNP concentration (Fig. 3). Urtizbera et al. have reported that, as the ferrofluid concentration increases, the alignment of magnetic moments along the external field gets hindered, as evidenced by the dependency of the dc magnetization curves on ferrofluid concentration [16]. Although Dutz and Hergt used particles with diameters of 20–50 nm, which were larger than the  $11 \pm 3$  nm particles used in this study, they also observed a decrease in magnetization with increases in concentration of packed MNPs [18]. Urtizbera et al. have explained their result using the numerical simulations in Ref. 15 for cases of high and moderate

anisotropy [15, 16]. It is a conventional model for representing dipole–dipole interaction and can be applied to single-domain MNPs. The model of Ref. 15 was used for this study, because the particle diameter used and the dependence of dc magnetization on MNP concentration were similar to those in the report by Urtizbera et al. [16]. The strength of the dipole–dipole interaction increases with MNP concentration [16, 18, 19]; therefore, we can conclude that, in our study, the magnetization decreased because of the increase in dipole–dipole interactions associated with higher concentrations of MNPs.

### B. ILP and ac hysteresis loops

Figure 4 shows the dependence of ac hysteresis loops on the concentration of MNPs at 5 and 500 kHz. Magnetization declined with increases in concentration at 5 kHz, as with the dc hysteresis loops [Fig. 4 (a)]. Except for the sample of 37 mg-Fe/ml, the difference of magnetization depending on the MNP concentration was marginal at 500 kHz [Fig. 4 (b)]. It is indicated that the difference in the amplitude of the rotation of magnetic moments was marginal in the higher concentration with the higher frequency. Figure 5 shows a comparison of the ac hysteresis loop for the liquid and fixed samples, both with 37 mg-Fe/ml concentration. The ac hysteresis loops had larger hysteresis areas than the dc hysteresis loops for both the liquid and fixed samples. When the rotation of magnetic moments was slow compared with the frequency of the applied magnetic field, the samples showed anisotropic behavior, characterized by the larger hysteresis area. In the fixed sample, contribution of Néel relaxation to heat dissipation was confirmed, because the ac hysteresis loop of the fixed sample had hysteresis areas for both 5 and 500 kHz. Coercivity of the liquid sample was larger than that of the fixed sample. This indicates that both Brownian and Néel relaxation occurred in the liquid sample [21]. The amplitude of particle rotation decreased and the phase delay in the rotation of magnetic moment increased with increase of frequency, which is indicated by the decrease of magnetization in the liquid sample and the increase of coercivity in the fixed sample, respectively (Fig. 5). Therefore, Brownian relaxation was dominant at the lower frequency whereas Néel relaxation gradually occurred at the higher frequency. Figure 6 shows the dependence of ac hysteresis loops on frequency at 37 mg-Fe/ml in the liquid sample. Magnetization decreased with increase of frequency because the rotations of particles and magnetic moments gradually delay with increase of frequency [20].

The dependence of ILP on frequency, as estimated from the areas of the ac hysteresis loops, is shown in Fig. 7. In the liquid samples, the frequency of the relaxation peak increased with decreases in MNP concentration. These relaxation peaks were Brownian relaxation peaks because these peaks were not confirmed in the fixed sample (Fig. 7). Additionally, the peak frequency of Brownian relaxation  $f_B$  calculated using Eq. (1) is 3.4 kHz ( $\eta = \eta_{\text{water}} = 0.89 \text{ mPa}\cdot\text{s}$ ). The measured frequency of the Brownian relaxation peak is in good agreement with the calculated frequency. However, the influence of MNP concentration on Brownian relaxation time is not considered in conventional theoretical models for magnetic relaxation [Eq. (1)]. For higher concentrations of MNPs, dipole–dipole interactions inhibit particle rotation. The strength of dipole–dipole interactions increases with decreases in interparticle distance for higher concentrations of MNPs [22, 23], and the rotation of particles is inhibited at higher concentrations. Thus, the Brownian relaxation time is short for lower concentrations of MNPs because of the rotatable state of particles with lower dipole–dipole interactions. With respect to the fixed sample, ILP increased with frequency because the rotation of magnetic moments was gradually delayed with the increases of frequency (Fig. 5). The frequency of Néel relaxation peak  $f_N$  was not observed in Fig. 7. It was assumed that Néel relaxation was dominant at higher

frequency than 1–500 kHz of the measuring frequency range. The theoretical  $f_N$  is higher than 450 kHz [Eq. (2);  $K \leq 41$  kJ/m<sup>3</sup>] [6, 8, 24]. It has been reported that  $\chi''$  decreases with increases in MNP concentration because of dipole–dipole interactions [14]. Using Eqs. (4) and (5), ILP is obtained as follows:

$$ILP = \frac{\mu_0 \pi \chi''}{\rho} = \frac{\mu_0 \pi \chi''_w}{v} \quad (6)$$

where  $\chi''_w$  and  $v$  were the imaginary part of susceptibility per mass and the volume of the measured sample, respectively. In conventional study,  $\chi''_w$  was used as  $\chi''$ . As  $v$  is constant, ILP is proportional to  $\chi''_w$ . Figure 7 shows that ILP decreased with increases in MNP concentration for higher frequencies in which Néel relaxation gradually dominated. This is in good agreement with the dependency of  $\chi''$  on the MNP concentration in the conventional model [15]. Since magnetization in the higher concentration in the liquid sample was similar to each other, the decrease of ILP in the higher concentration was associated with the shorter phase delay in the particle rotation. Therefore, the decrease in ILP can be associated with the inhibition of the rotation of magnetic moment due to dipole–dipole interactions. The decrease in heat dissipation with the higher MNP concentrations has also been confirmed by the calorimetric measurements of SLP [17, 25].

In the higher frequency, ILP of the liquid sample was higher than that of the fixed sample in spite of the reduction of Brownian relaxation. This was indicated that the particle rotation was slightly remained in the higher frequency, which was confirmed by the measurement of ac hysteresis loops (Fig. 5). Magnetization in the liquid sample was higher than that in the fixed sample, which represented the particle rotation in the higher frequency. Thus, the delay of the particle rotation occurred, and coercivity of the liquid sample was higher than that of the fixed sample.

#### IV. Conclusion

Greater dipole–dipole interactions with increases in MNP concentration were confirmed by measurement of dc and ac hysteresis loops. Magnetization decreased with the increase of MNP concentration because the strength of dipole–dipole interaction increased in the higher MNP concentration. Through measurement of ac hysteresis loops and assessment of ILP, the increase in Brownian relaxation peak frequency with the decrease in MNP concentration was confirmed. The rotation of particles was inhibited with the higher concentrations because of dipole–dipole interactions. Moreover, the heat dissipation, as estimated from hysteresis loops, decreased with the increases in MNP concentration because of the inhibition of the rotation of magnetic moment with increases in dipole–dipole interactions.

#### References

- <sup>1</sup> Q. A. Pankhurst, J. Connolly, S. K. Jones, and J. Dobson, *J. Phys. D: Appl. Phys.* **36**, R167 (2003).
- <sup>2</sup> R. M. Ferguson, K. R. Minard, and K. M. Krishnan, *J. Magn. Magn. Mater.* **321**, 1548 (2009).
- <sup>3</sup> Y. Liu, H. Miyoshi, and M. Nakamura, *Int. J. Cancer* **120**, 2527 (2007).
- <sup>4</sup> K. Hayashi, M. Nakamura, W. Sakamoto, T. Yogo, H. Miki, S. Ozaki, M. Abe, T. Matsumoto, and K. Ishimura, *Theranostics* **3**, 366 (2013).
- <sup>5</sup> D. Kami, T. Kitani, T. Kishida, O. Mazda, M. Toyoda, A. Tomitaka, S. Ota, R. Ishii, Y. Takemura, M. Watanabe, A. Umezawa, and S. Gojo, *Nanomed.: Nanotechnol. Biol. Med.* **10**, 1165 (2014).

- <sup>6</sup> R. E. Rosensweig, *J. Magn. Magn. Mater.* **252**, 370 (2002).
- <sup>7</sup> S. Purushotham and R.V. Ramanujan, *J. Appl. Phys.* **107**, 114701 (2010).
- <sup>8</sup> P. C. Fannin, C. N. Marin, and C. Couper, *J. Magn. Magn. Mater.* **322**, 1677 (2010).
- <sup>9</sup> J. Carrey, B. Mehdaoui, and M. Respaud, *J. Appl. Phys.* **109**, 083921 (2010).
- <sup>10</sup> J. Zhang, C. Boyd, and W. Luo, *Phys. Rev. Lett.* **77**, 390 (1996).
- <sup>11</sup> S. H. Chung, A. Hoffmann, S. D. Bader, C. Liu, B. Kay, L. Makowski, and L. Chen, *Appl. Phys. Lett.* **85**, 2971 (2004).
- <sup>12</sup> R. Hergt, S. Dutz, R. Müller, and M. Zeisberger, *J. Phys.: Condens. Matter.* **18**, S2019 (2006).
- <sup>13</sup> M. Kallumadil, M. Tada, T. Nakagawa, M. Abe, P. Southern, and Q. A. Pankhurst, *J. Magn. Magn. Mater.* **321**, 1509 (2009).
- <sup>14</sup> R. Hergt and S. Dutz, *J. Magn. Magn. Mater.* **311**, 187 (2007).
- <sup>15</sup> D. V. Berkov and N. L. Gorn, *J. Phys.: Condens. Matter.* **13**, 1 (2001).
- <sup>16</sup> A. Urtizberea, E. Natividad, A. Arizaga, M. Castro, and A. Mediano, *J. Phys. Chem. C* **114**, 4916 (2010).
- <sup>17</sup> D. Serantes, D. Baldomir, C. Martinez-Boubeta, K. Simeonidis, and M. Angelakeris, *J. Appl. Phys.* **108**, 073918 (2010).
- <sup>18</sup> S. Dutz and R. Hergt, *J. Nano-Electron. Phys.* **4**, 02010-1 (2012).
- <sup>19</sup> C. Haase and U. Nowak, *Phys. Rev. B* **85**, 045435 (2012).
- <sup>20</sup> K. Nakamura, K. Ueda, A. Tomitaka, T. Yamada, and Y. Takemura, *IEEE Trans. Magn.*, **49**, 1 (2013).
- <sup>21</sup> A. Tomitaka, K. Ueda, T. Yamada, and Y. Takemura, *J. Magn. Magn. Mater.* **324**, 3437 (2012).
- <sup>22</sup> M. F. Hansen and S. Mørup, *J. Magn. Magn. Mater.* **184**, 262 (1998).
- <sup>23</sup> J. García-Otero, M. Porto, J. Rivas, and A. Bunde, *Phys. Rev Lett.* **84**, 167 (2000).
- <sup>24</sup> M. Suto, Y. Hirota, H. Mamiya, A. Fujita, R. Kasuya, K. Tohji, and B. Jeyadevan, *J. Magn. Magn. Mater.* **321**, 1493 (2009).
- <sup>25</sup> P. H. Linh, P. V. Thac, N. A. Tuan, N. C. Thuan, D. H. Manh, N. X. Phuc, and L. V. Hong, *J. Phys.: Conf. Ser.* **187**, 012069 (2009).

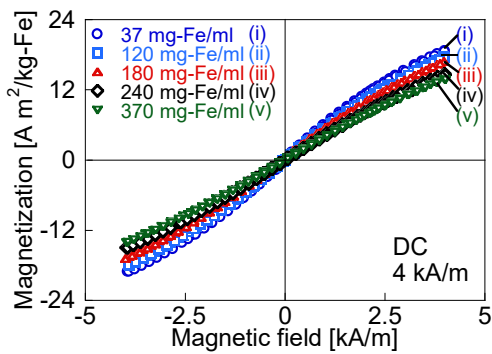


Fig. 1 The dependence of dc hysteresis loops in the liquid samples on concentration of MNPs. The applied magnetic field was 0–4 kA/m. The MNP concentration was (i) 37, (ii) 120, (iii) 180, (iv) 240, and (v) 370 mg-Fe/ml.

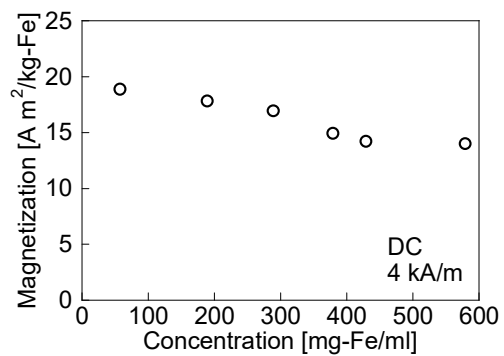


Fig. 3 The dependence of the maximum magnetization of dc hysteresis loops in Fig. 1 on MNP concentration.

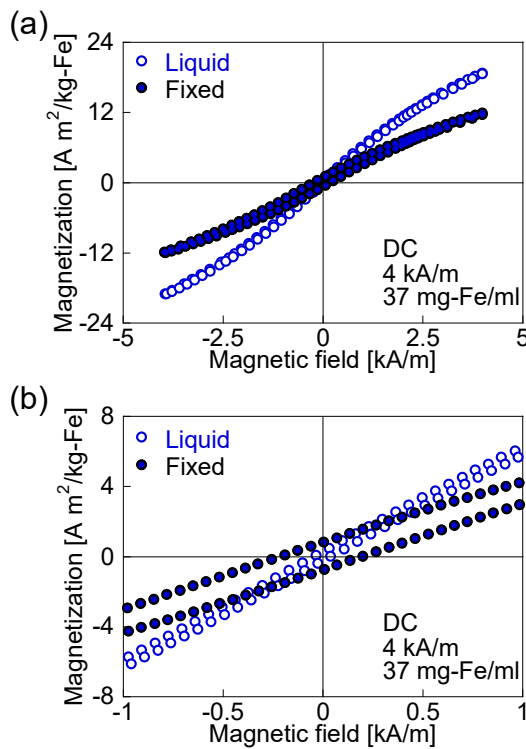


Fig. 2 (a) Dc hysteresis loops of the liquid and fixed samples at 0–4 kA/m of amplitude of magnetic field. (b) Magnification of (a).

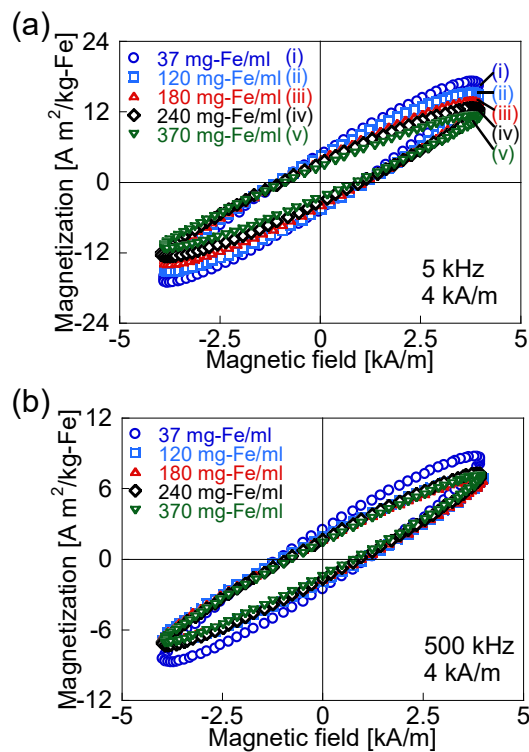


Fig. 4 The dependence of ac hysteresis loops in the liquid samples on MNP concentration. The amplitude of the applied magnetic field was 4 kA/m. The frequency was (a) 5 and (b) 500 kHz. The MNP concentration was (i) 37, (ii) 120, (iii) 180, (iv) 240, and (v) 370 mg-Fe/ml.

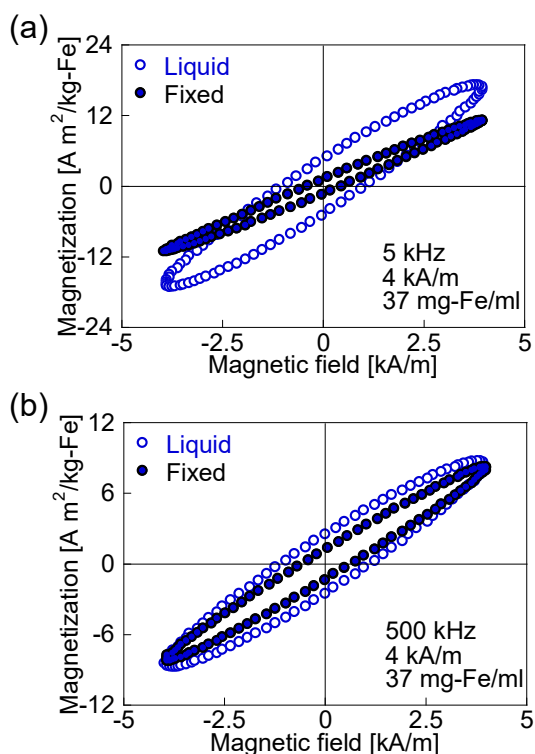


Fig. 5 Ac hysteresis loops of the liquid and fixed samples at 4 kA/m amplitude of applied magnetic field. The frequency was (a) 5 kHz and (b) 500 kHz.

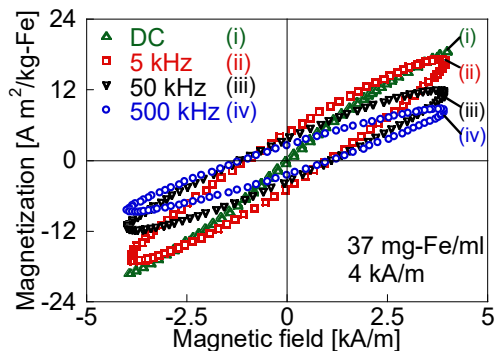


Fig. 6 (i) Dc and (ii–iv) ac hysteresis loops at (ii) 5, (iii) 50, and (iv) 500 kHz. Amplitude of the applied magnetic field was 4 kA/m.

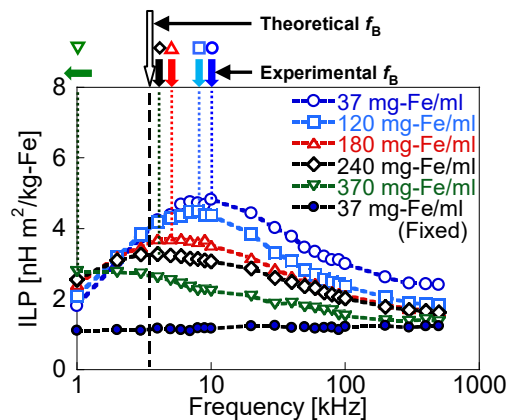


Fig. 7 Dependence of ILP on frequency for the liquid and fixed samples. The liquid samples had MNP concentrations of 37–370 mg-Fe/ml. The fixed sample had MNP concentration of 37 mg-Fe/ml. Dotted line shows the theoretical Brownian relaxation time  $f_B = 3.4$  kHz. The arrows above this graph show the experimental  $f_B$  in each MNP concentration. The experimental  $f_B$  was 4, 5, 8, and 10 kHz in the MNP concentration of 240, 180, 120, and 37 mg-Fe/ml, respectively. In terms of 370 mg-Fe/ml,  $f_B$  was lower than 1 kHz.